

# Semi-empirical PM3 calculations predict the fluorescence quantum yields ( $\Phi$ ) of 4-monosubstituted benzofurazan compounds

2 PERKIN

Seiichi Uchiyama, Tomofumi Santa, Natsuko Okiyama, Kentaro Azuma and Kazuhiro Imai\*

Graduate School of Pharmaceutical Sciences, The University of Tokyo, 7-3-1 Hongo, Bunkyo-ku, Tokyo 113-0033, Japan. E-mail: kimai@mol.f.u-tokyo.ac.jp; Fax: 81-3-5841-4885

Received (in Cambridge, UK) 10th January 2000, Accepted 27th March 2000

Published on the Web 15th May 2000

We have elucidated the relationship between the fluorescence quantum yield ( $\Phi$ ) of 4-monosubstituted benzofurazan (2,1,3-benzoxadiazole) compounds and the substituent group at the 4-position using a group of eleven such compounds. The absorption and fluorescence spectra of these compounds were measured in fifteen different solvents. Semi-empirical PM3 calculations were carried out to obtain the optimized geometry, energies, charges and dipole moments of this group in the ground and excited states. The  $S_1$ - $T_2$  energy gaps obtained from the PM3-CAS/CI calculations, which reflected the probability of  $S_1 \rightarrow T_2$  intersystem crossing, related well to the fluorescence quantum yield ( $\Phi$ ) of the 4-monosubstituted benzofurazan compounds in nonpolar solvents. It also appeared that the decrease in the  $S_1$ - $T_1$  energy gaps was related to the change in the fluorescence quantum yield ( $\Phi$ ) due to solvent effects. In highly polar solvents, non-radiative  $S_1 \rightarrow T_1$  intersystem crossing occurs, in addition to non-radiative  $S_1 \rightarrow T_2$  intersystem crossing, in 4-monosubstituted benzofurazan compounds, as they have a larger dipole moment in the  $S_1$  state than in the  $T_2$  state. These studies have enabled us to predict the fluorescence quantum yield ( $\Phi$ ) for a series of 4-monosubstituted benzofurazan compounds.

## Introduction

Elucidation of a general relationship between fluorescence characteristics (the maximum excitation/emission wavelengths and fluorescence quantum yield ( $\Phi$ )) and chemical structure has been of great interest to scientists in the fields of analytical and biological chemistry. In particular, the relationship between substituent groups and  $\Phi$  of the fluorophore (for example, coumarin, fluorescein, pyrene, naphthalene and bodipy) is quite important for developing fluorescent derivatization reagents,<sup>1</sup> fluorescent probes and fluorescent ion sensors.<sup>2</sup> There have been many reports on the effects of substituent groups on the fluorescence characteristics of molecules with coumarin,<sup>3</sup> naphthalene,<sup>4</sup> thioxanthone,<sup>5</sup> coelenteramine analogues (2-acetamido-3-benzyl-5-pyrazine),<sup>6</sup> carbostyryl (quinolin-2(1*H*)-ones)<sup>7</sup> or imidazo[1,2-*a*]pyridine<sup>8</sup> skeletons. In spite of this, we do not have any practical rules which precisely predict the fluorescence quantum yield ( $\Phi$ ) of a series of compounds based on their chemical structure.

The benzofurazan (2,1,3-benzoxadiazole, **1**) skeleton is one of the most popular fluorophores. Uniquely, the fluorescence characteristics of this fluorophore are dramatically changed by substituent groups at the 4- and/or 7-positions.<sup>9</sup> Many "fluorogenic reagents", which are non-fluorescent themselves and react with analytes to form fluorescent derivatives, such as 4-fluoro-7-nitro-2,1,3-benzoxadiazole (NBD-F),<sup>10</sup> 4-(*N,N*-dimethylaminosulfonyl)-7-fluoro-2,1,3-benzoxadiazole (DBD-F),<sup>11</sup> 4-aminosulfonyl-7-fluoro-2,1,3-benzoxadiazole (ABD-F)<sup>12</sup> and 7-fluoro-2,1,3-benzoxadiazole-4-sulfonate (SBD-F)<sup>13</sup> have been developed. In a previous report,<sup>9</sup> we synthesized seventy 4,7-disubstituted benzofurazan compounds and investigated the effects of the substituent groups at the 4- and 7-positions on their fluorescence characteristics in methanol. As a result, we found a relationship between the fluorescence characteristics and the Hammett substituent constants ( $\sigma_p$ )<sup>14,15</sup> of the substituent groups at the 4- and 7-positions. Similarly, the relationship between the fluorescence characteristics, the electronic density and the dipole moment directed from the 4- to the 7-position

were obtained by semi-empirical PM3<sup>16,17</sup> calculations.<sup>18</sup> These relationships enabled us to approximately predict the fluorescence characteristics of 4,7-disubstituted benzofurazan compounds, and we have developed new fluorogenic reagents based on these relationships.<sup>19-21</sup> We also showed with PM3-CAS/CI calculations that the probability of non-radiative  $S_1 \rightarrow T_2$  intersystem crossing influenced  $\Phi$  of six fluorescent 4,7-disubstituted benzofurazan compounds.<sup>22</sup> However, in a previous report, the probabilities of other non-radiative transitions were ignored because of the complexity of the 4,7-disubstituted benzofurazan compounds. Furthermore, there were no arguments about the solvent effects on  $\Phi$ . To solve these issues, first of all, a theoretical study on  $\Phi$  of more simplified benzofurazan compounds was necessary.

In this article, we have selected a series of eleven 4-monosubstituted benzofurazan compounds **1-11** and tried to theoretically elucidate the relationship between  $\Phi$  of these compounds and the substituent groups at the 4-position. First, the absorption and fluorescence spectra of the compounds were obtained in fifteen solvents. In addition, semi-empirical PM3 calculations were performed on the compounds to obtain optimized geometry, energies, charge distributions and dipole moments in their ground and excited states. Comparing the experimental results with computational results, we have discussed the effects of the 4-substituent on  $\Phi$  of the benzofurazan compounds in non-polar and polar solvents.

## Results and discussion

### Fluorescence characteristics and PM3-CAS/CI calculations of non-/mono-substituted benzofurazan compounds

Eleven 4-monosubstituted benzofurazan compounds (**1-11**) were synthesized, to study the effects of the 4-substituent on fluorescence characteristics. The maximum absorption and emission wavelengths and the fluorescence quantum yields ( $\Phi$ ) of **1-11** in various solvents are summarized in Table 1. These results showed that the fluorescence character-

**Table 1** Fluorescence characteristics of mono-substituted benzofurazan compounds; maximum absorption wavenumber ( $\nu_{ab}$ ), maximum emission wavenumber ( $\nu_{em}$ ), Stokes shift ( $\Delta\nu$ ) and fluorescence quantum yield ( $\Phi$ )

No.	Solvent	<b>1</b>		<b>2</b>			<b>3</b>				
		$10^{-3} \nu_{ab}/\text{cm}^{-1}$	$\Phi$	$10^{-3} \nu_{ab}/\text{cm}^{-1}$	$10^{-3} \nu_{em}/\text{cm}^{-1}$	$10^{-3} \Delta\nu/\text{cm}^{-1}$	$10^{-3} \nu_{ab}/\text{cm}^{-1}$	$10^{-3} \nu_{em}/\text{cm}^{-1}$	$10^{-3} \Delta\nu/\text{cm}^{-1}$	$\Phi$	
1	<i>n</i> -Hexane	—	—	24.8	19.5	5.3	0.15	26.6	20.0	6.6	0.047
2	Cyclohexane	—	—	24.8	19.4	5.4	0.17	26.8	19.8	7.0	0.053
3	Carbon tetrachloride	—	—	24.3	19.1	5.2	0.13	26.3	19.4	6.9	0.040
4	Diethyl ether	33.7	—	24.2	19.1	5.1	0.13	25.3	19.1	6.2	0.043
5	Benzene	32.6	—	23.8	18.7	5.1	0.10	25.8	19.3	6.5	0.038
6	1,4-Dioxane	32.9	—	23.8	18.3	5.5	0.076	25.1	18.8	6.3	0.023
7	Dichloromethane	33.1	—	23.6	17.7	5.9	0.030	25.7	18.9	6.8	0.015
8	Ethyl acetate	33.3	—	23.7	18.3	5.4	0.062	25.2	18.8	6.4	0.019
9	Tetrahydrofuran	33.2	—	23.8	18.4	5.4	0.063	24.8	18.8	6.0	0.027
10	Acetone	—	—	23.6	17.7	5.9	0.030	24.8	18.2	6.6	0.010
11	Acetonitrile	33.1	—	23.6	17.3	6.3	0.010	25.1	17.9	7.2	0.0052
12	Propan-2-ol	33.3	—	24.0	17.3	6.7	0.0013	24.9	17.4	7.5	0.00038
13	Ethanol	33.3	—	24.0	17.1	6.9	0.00074	24.8	17.2	7.6	0.00016
14	Methanol	33.3	—	23.8	16.8	7.0	0.000039	24.9	17.2	7.7	0.00015
15	Water	32.9	—	24.3	—	—	—	26.0	—	—	—

No.	<b>4</b>				<b>5</b>				<b>6</b>			
	$10^{-3} \nu_{ab}/\text{cm}^{-1}$	$10^{-3} \nu_{em}/\text{cm}^{-1}$	$10^{-3} \Delta\nu/\text{cm}^{-1}$	$\Phi$	$10^{-3} \nu_{ab}/\text{cm}^{-1}$	$10^{-3} \nu_{em}/\text{cm}^{-1}$	$10^{-3} \Delta\nu/\text{cm}^{-1}$	$\Phi$	$10^{-3} \nu_{ab}/\text{cm}^{-1}$	$10^{-3} \nu_{em}/\text{cm}^{-1}$	$10^{-3} \Delta\nu/\text{cm}^{-1}$	$\Phi$
1	27.6	23.1	4.5	0.47	27.6	21.9	5.7	0.0023	30.2	24.3	5.9	0.0022
2	27.5	22.9	4.6	0.53	27.4	21.7	5.7	0.0024	30.0	24.1	5.9	0.0026
3	27.2	22.4	4.8	0.80	27.2	21.1	6.1	0.0018	29.6	23.7	5.9	0.0059
4	27.3	22.1	5.2	0.68	27.3	20.5	6.8	0.00057	29.7	23.1	6.6	0.0059
5	26.8	21.5	5.3	0.64	27.0	19.9	7.1	0.00062	29.2	22.9	6.3	0.0092
6	27.0	21.3	5.7	0.68	27.1	19.8	7.3	0.00042	29.3	22.6	6.7	0.012
7	26.8	21.2	5.6	0.62	27.0	19.3	7.7	0.00024	29.2	22.3	6.9	0.012
8	27.0	21.4	5.6	0.49	27.2	19.7	7.5	0.00031	29.3	22.7	6.6	0.010
9	26.9	21.3	5.6	0.54	27.0	19.6	7.4	0.00028	29.2	22.6	6.6	0.010
10	26.9	20.6	6.3	0.48	27.1	19.2	7.9	0.00013	29.3	22.2	7.1	0.011
11	27.0	20.3	6.7	0.42	27.0	18.9	8.1	0.00012	29.2	21.9	7.3	0.012
12	27.1	19.9	7.2	0.36	27.2	20.1	7.1	0.00030	29.4	21.7	7.7	0.012
13	27.0	19.7	7.3	0.27	27.2	19.7	7.5	0.00020	29.4	21.4	8.0	0.011
14	27.0	19.5	7.5	0.20	27.1	18.9	8.2	0.00012	29.2	21.2	8.0	0.012
15	26.7	18.7	8.0	0.015	27.0	—	—	—	28.9	19.6	9.3	0.0065

No.	<b>7</b>				<b>8</b>		<b>9</b>		<b>10</b>		<b>11</b>	
	$10^{-3} \nu_{ab}/\text{cm}^{-1}$	$10^{-3} \nu_{em}/\text{cm}^{-1}$	$10^{-3} \Delta\nu/\text{cm}^{-1}$	$\Phi$	$10^{-3} \nu_{ab}/\text{cm}^{-1}$	$\Phi$	$10^{-3} \nu_{ab}/\text{cm}^{-1}$	$\Phi$	$10^{-3} \nu_{ab}/\text{cm}^{-1}$	$\Phi$	$10^{-3} \nu_{ab}/\text{cm}^{-1}$	$\Phi$
1	28.7	22.8	5.9	0.084	33.0	—	33.6	—	32.8	—	31.9	—
2	28.6	22.8	5.8	0.074	33.0	—	33.3	—	32.6	—	32.1	—
3	28.5	22.4	6.1	0.081	32.4	—	33.2	—	32.5	—	31.4	—
4	28.2	22.3	5.9	0.087	32.2	—	33.2	—	32.6	—	31.4	—
5	28.2	22.1	6.1	0.10	31.5	—	34.5	—	32.3	—	31.0	—
6	28.0	21.8	6.2	0.081	31.8	—	33.1	—	32.4	—	31.2	—
7	28.3	21.7	6.6	0.067	32.1	—	33.0	—	32.4	—	31.1	—
8	28.2	21.8	6.4	0.10	31.9	—	32.9	—	32.5	—	31.3	—
9	27.9	21.8	6.1	0.077	31.6	—	33.1	—	32.3	—	31.1	—
10	28.1	21.4	6.7	0.076	—	—	—	—	—	—	—	—
11	28.2	21.3	6.9	0.070	31.9	—	33.1	—	32.6	—	31.1	—
12	28.7	20.5	8.2	0.058	32.4	—	33.1	—	32.5	—	31.3	—
13	28.6	20.4	8.2	0.044	32.2	—	32.9	—	32.4	—	31.3	—
14	28.7	20.0	8.7	0.033	32.1	—	33.1	—	32.5	—	31.3	—
15	29.4	19.2	10.2	0.0026	31.6	—	33.0	—	32.3	—	30.7	—

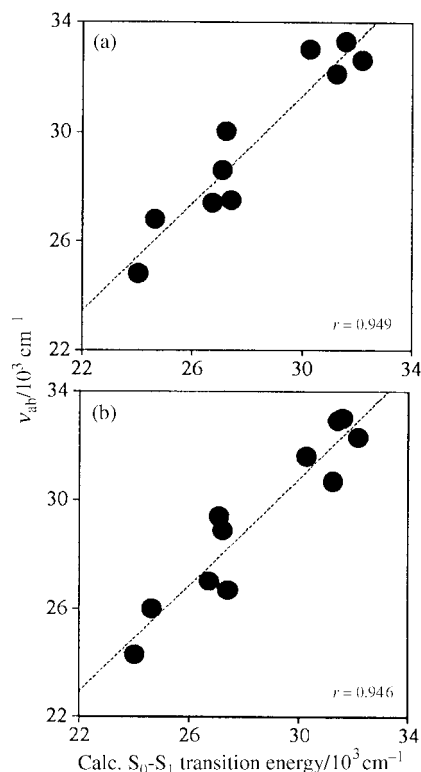
istics of these compounds were affected by variation in the 4-substituent.

To elucidate this relationship PM3-CAS/CI calculations were carried out. The probability of non-radiative transitions, such as the internal conversion and the intersystem crossing, can be estimated by this PM3-CAS/CI calculation because it can provide us with not only the energies of the singlet states, but also of the triplet states. The calculation results, using the geometrically optimized 4-monosubstituted benzofurazan compounds, are shown in Table 2. As a first step, the

correlation between the experimental liquid-phase absorption maximum and calculated  $S_0 \rightarrow S_1$  (mainly, HOMO  $\rightarrow$  LUMO) transition energies was made (Fig. 1). This correlation is not strictly valid because we ignored vibration and solvent effects. Nevertheless, a good correlation was obtained because of the vibration and the solvent effects for all compounds in the set are similar. This good correlation also indicated that the absorption occurred with the HOMO  $\rightarrow$  LUMO electronic transition. As PM3-CAS/CI calculation seemed to reflect the electronic properties of the 4-monosubstituted benzofurazan

**Table 2** Calculated properties of 4-monosubstituted benzofurazan compounds

Compound	$H_f/\text{kcal mol}^{-1}$	Energy relative to $S_0/\text{cm}^{-1}$				$\mu(S_0)/D$	$\mu(T_1)/D$	$\mu(S_1)/D$	$\mu(T_2)/D$	$a/10^8 \text{ cm}^a$
		$T_1$	$S_1$	$T_2$	Others					
1	102.88	18153	31415	27262	30607 $^3(n,\pi^*)$ 31613 $^1(n,\pi^*)$	3.88	6.01	4.89	4.95	2.79
2	101.15	15115	24048	25493	—	4.25	7.72	10.16	6.29	3.61
3	100.09	15051	24659	25495	—	3.97	7.04	8.93	5.66	2.95
4	104.71	16870	27404	30774	17481 $^3(n,\pi^*)$ 24827 $^1(n,\pi^*)$	5.03	5.60	11.42	6.93	3.80
5	140.25	18078	26733	24729	—	5.22	9.71	11.57	3.06	4.98
6	65.74	15698	27229	25902	—	4.88	8.44	8.12	6.68	3.59
7	58.88	16429	27083	26487	—	1.92	5.77	7.27	5.11	4.31
8	61.77	17714	30264	27230	30444 $^3(n,\pi^*)$ 32585 $^1(n,\pi^*)$	3.90	6.38	2.63	5.02	2.80
9	41.47	18398	31586	27488	—	4.51	4.72	5.15	3.30	3.78
10	77.06	19341	32175	29322	29996 $T_3$	5.00	5.20	5.58	6.03	4.53
11	99.23	18242	31244	27635	31180 $^3(n,\pi^*)$ 32958 $^1(n,\pi^*)$	5.65	6.08	7.08	5.59	3.09

<sup>a</sup> Onsager cavity.**Fig. 1** The relationships between the calculated  $S_0$ - $S_1$  transition energy and the experimental maximum absorption wavelengths of 4-monosubstituted benzofurazan compounds in (a) cyclohexane, (b) water.

compounds, we used the PM3-CAS/CI method in the following study.

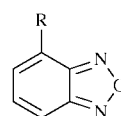
#### The effects of the substituent group at the 4-position on the fluorescence quantum yields ( $\Phi$ ) of 4-monosubstituted benzofurazan compounds in non-polar solvents

We first tried to elucidate the relationship between  $\Phi$  of 1–11 in non-polar solvents and their substituents. Cyclohexane was selected as a representative non-polar solvent. The fluorescence characteristics of these compounds in cyclohexane (Table 1) indicated that the  $\Phi$  values are indeed determined by the variation in substituent group. We considered that these differences in  $\Phi$  were based on the differences in the probability of non-radiative transitions, because no photochemical reactions were observed for any of the compounds (the fluorescence intensities did not change during the measurement), therefore, the probability of internal conversion and intersystem crossing were estimated.

For the occurrence of  $S_1 \rightarrow S_0$  internal conversion, proximity

**Table 3** Calculated maximum vibrational energies of 4-monosubstituted benzofurazan compounds

Compound	Energy/ $\text{cm}^{-1}$	Attribution
1	3076	C–H stretching in benzofurazan skeleton
2	3135	C–H stretching in substituent group
3	3536	N–H stretching in substituent group
4	3193	C–H stretching in substituent group
5	3079	C–H stretching in benzofurazan skeleton
6	3143	C–H stretching in substituent group
7	3370	N–H stretching in substituent group
8	3076	C–H stretching in benzofurazan skeleton
9	3216	C–H stretching in substituent group
10	3075	C–H stretching in benzofurazan skeleton
11	3070	C–H stretching in benzofurazan skeleton

**Fig. 2** Structural changes of 4-monosubstituted benzofurazan compounds investigated in this study; (a) twisting of the substituent group, (b) wagging of the benzofurazan skeleton.

- 1 R = H
- 2 R = NMe<sub>2</sub>
- 3 R = NH<sub>2</sub>
- 4 R = SMe
- 5 R = SPh
- 6 R = OMe
- 7 R = NHCOMe
- 8 R = F
- 9 R = SO<sub>2</sub>Me
- 10 R = SO<sub>2</sub>Ph
- 11 R = NO<sub>2</sub>

of the  $S_1$  state to the  $S_0$  state in the excited state is necessary.<sup>23</sup> We first calculated the energies of the molecular vibrations, such as stretching and bending, with the PM3 method. The maximum vibrational energies obtained with PM3 calculations are summarized in Table 3. These were small in comparison with the calculated  $S_1$ - $S_0$  energy gaps (Tables 1 and 2), indicating that the  $S_1$  state is sufficiently separate from the  $S_0$  state that the  $S_1 \rightarrow S_0$  internal conversion does not occur. Next we focused on macro-structural changes. According to a previous report,<sup>24</sup> twisting of the substituent group and distortion of the fluorophore lead to an energetically low excited state. In particular, the transition to the twisted intramolecular charge transfer (TICT) state<sup>25</sup> with a twist of the substituent group has been reported as an important non-radiative pathway, even in non-polar solvents.<sup>26</sup> The influence of these structural changes (Fig. 2) on the energies of the  $S_0$  and  $S_1$  states was studied for compounds 1–11. The results obtained with the PM3-CAS/CI are shown in

**Table 4** Effect of molecular geometry on  $S_0$  and  $S_1$  energy levels<sup>a</sup>

	1	2	3	4	5	6	7	8	9	10	11
Substitutional rotation											
$S_0$ (plane)/ $\text{cm}^{-1}$	—	-2904	-3049	-1500	-855	-2387	-3000	—	-2097	-2000	-2073
$S_1$ (plane)/ $\text{cm}^{-1}$	—	21777	22003	25027	26414	26423	23479	—	19317	30713	29028
$S_1-S_0$ (plane)/ $\text{cm}^{-1}$	—	24681	25052	26527	27269	28810	26479	—	21414	32713	31101
$S_0$ (twist)/ $\text{cm}^{-1}$	—	-2742	-2871	-2258	-823	-2758	-1831	—	-2565	-1887	-2879
$S_1$ (twist)/ $\text{cm}^{-1}$	—	26777	26664	29423	(31036) <sup>b</sup>	27963	28286	—	29431	30560	29036
$S_1-S_0$ (twist)/ $\text{cm}^{-1}$	—	29519	29535	31681	(31859)	30721	30117	—	31996	32447	31915
Ring distortion											
$S_0$ (plane)/ $\text{cm}^{-1}$	-2881	-2863	-3089	-1468	-855	-2387	-1565	-2766	-2210	-1823	-2742
$S_1$ (plane)/ $\text{cm}^{-1}$	28939	21664	22019	26229	26431	26423	24592	27882	29915	30608	29028
$S_1-S_0$ (plane)/ $\text{cm}^{-1}$	26058	24527	25108	27697	27286	28810	26157	30648	32125	32431	31170
$S_0$ (twist)/ $\text{cm}^{-1}$	-2399	-2250	-2468	-1887	-557	-2597	-2299	-2428	-2097	-613	-2274
$S_1$ (twist)/ $\text{cm}^{-1}$	16615	16042	15107	18115	19833	15671	15929	16373	19317	27713	18647
$S_1-S_0$ (twist)/ $\text{cm}^{-1}$	14276	18292	17575	20002	20390	18268	18228	18801	21414	28326	20921

<sup>a</sup> For compounds **4**, **5**, **6**, **7**, **9** and **10**, having two stable planar geometries, the energies at the geometry with the more stable  $S_0$  were described. However, this alternative makes no difference. <sup>b</sup> Under this state, there was another singlet state ( $25245 \text{ cm}^{-1}$ ) which was  $S_2$  with planar geometry.

**Table 5** Energy gaps between  $S_1$  and  $T_n$  ( $n = 1, 2$ )

	1	2	3	4	5	6	7	8	9	10	11
Optimized for $S_0$											
$S_1-T_2/\text{cm}^{-1}$	4153	-1445	-836	-3370	2004	1327	596	3034	4098	2853	3609
$S_1-T_1/\text{cm}^{-1}$	13262	8933	9608	10534	8655	11531	10654	12550	13188	12834	13002
Optimized for $S_1$											
$S_1-T_2/\text{cm}^{-1}$	2513	-5515	-5408	-4209	-1966	-3455	-3201	4266	-7	-21348	-1956
$S_1-T_1/\text{cm}^{-1}$	14573	6765	6547	11548	7201	8254	10187	15531	10311	14096	9813

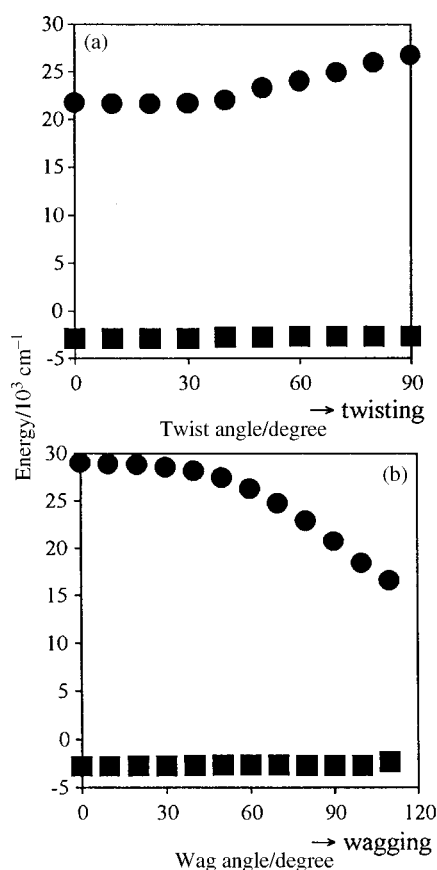


**Fig. 3** Effects of the structural changes on the  $S_0$  (■) and  $S_1$  (●) energies of 4-(*N,N*-dimethylamino)-2,1,3-benzoxadiazole (**2**) obtained with the PM3 calculation; (a) twisting of the  $\text{NMe}_2$  group, (b) wagging of benzofurazan skeleton.

Fig. 3 (a representative result) and Table 4. These results indicated that the twist of the substituent group is not favorable, because the energy of the  $S_1$  state for the twisted form is not smaller than that of the planar form. The wag of the benzofurazan skeleton, however, is favorable, because the  $S_1$  state is stabilized by this structural change, although despite this, the  $S_1-S_0$  energy gap for the wagging form was still too large to allow  $S_1 \rightarrow S_0$  internal conversion to occur. In summary,  $S_1 \rightarrow S_0$  internal conversion is not the main factor which causes the differences in  $\Phi$  for the compounds studied.

Next the probability of intersystem crossing was estimated. The calculated data (Table 2) showed that the  $T_2$  state was very close to the  $S_1$  state, and therefore, we obtained the  $S_1-T_1$  and  $S_1-T_2$  energy gaps (Table 5, for optimized  $S_0$  geometry). No significant relationships were found between the  $S_1-T_1$  energy gaps and  $\Phi$  of compounds **1–11** in cyclohexane. In contrast, the  $S_1-T_2$  energy gaps were clearly related to  $\Phi$  of these compounds in cyclohexane. The order of the  $S_1-T_2$  energy gap was **4** ( $-3370 \text{ cm}^{-1}$ ) < **2** ( $-1445$ ) < **3** ( $-836$ ) < **7** ( $596$ ) < **6** ( $1327$ ) < **5** ( $2004$ ) < **10** ( $2853$ ) < **8** ( $3034$ ) < **11** ( $3609$ ) < **9** ( $4098$ ) < **1** ( $4153$ ). This order was in good agreement with the order of  $\Phi$  in cyclohexane (**4** ( $\Phi = 0.53$ ) > **2** ( $0.17$ ) > **7** ( $0.074$ ) > **3** ( $0.053$ ) > **6** ( $0.0026$ ) > **5** ( $0.0024$ ) > **10**, **8**, **11**, **9**, **1** (not detected)). Considering that the  $S_1-T_2$  energy gap decreased for the  $S_1$  geometry (Table 5, for optimized  $S_1$  geometry), we inferred that the probability of  $S_1 \rightarrow T_2$  intersystem crossing was the maximum for the Franck-Condon state. If the  $T_2$  state lies above the  $S_1$  state (for e.g.  $R = \text{SMe}$  (**4**)) for the optimized  $S_0$  geometry, the  $S_1 \rightarrow T_2$  intersystem crossing is precluded and fluorescence occurs. In contrast, if the  $T_2$  state lies below the  $S_1$  state (for e.g.  $R = \text{SO}_2\text{Ph}$  (**10**),  $\text{F}$  (**8**),  $\text{NO}_2$  (**11**),  $\text{SO}_2\text{Me}$  (**9**)) for the optimized  $S_0$  geometry, fluorescence does not occur by the competitive  $S_1 \rightarrow T_2$  intersystem crossing. However, some of the excited molecules have a larger energy than the calculated  $S_1$  energy for the optimized  $S_0$  geometry because molecules vibrate and some

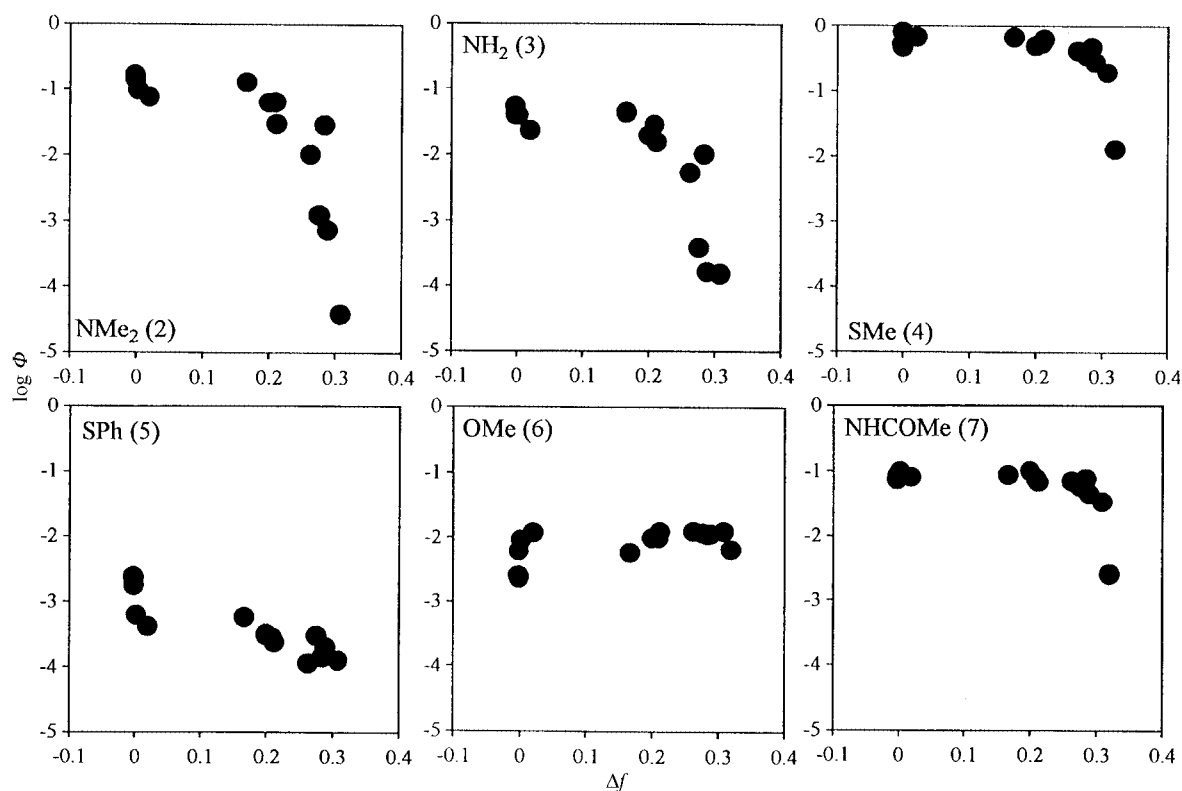


**Fig. 4** Dependence of the fluorescence quantum yields ( $\Phi$ ) of fluorescent 4-monosubstituted benzofurazan compounds on solvent polarity function  $\Delta f = (\epsilon - 1)/(2\epsilon + 1) - (n^2 - 1)/(2n^2 + 1)$ .

molecules are excited at a wavelength shorter than the maximum absorption wavelength. Therefore, the  $S_1 \rightarrow T_2$  intersystem crossing may occur even for  $R = SMe$  (4) or  $NMe_2$  (2). In short, these experimental and computational studies suggest that the difference in  $\Phi$  in compounds 1–11 in non-polar solvents is caused by the difference in the probability of the  $S_1 \rightarrow T_2$  intersystem crossing, which corresponds to the  $S_1-T_2$  energy gap. It has been reported that the fluorescence intensity of mono-substituted anthracene compounds was also determined by the  $S_1-T_2$  energy gaps.<sup>27,28</sup>

We propose a simple and useful method to predict the fluorescence characteristics of 4-substituted benzofurazan compounds in non-polar solvents. As the effects of the 4-substituent on  $\Phi$  of compounds 1–11 in non-polar solvents were revealed by the  $S_1-T_2$  energy gaps at the optimized  $S_0$  geometry obtained with the PM3-CAS/CI calculations, therefore, in general for 4-monosubstituted benzofurazan compounds, the PM3-CAS/CI calculations of the  $S_1-T_2$  energy gaps must correspond to the effects of the substituent group on  $\Phi$ . Furthermore, there was a tendency for the benzofurazan compound with the lower HOMO energy to have a larger  $\Phi$  value in non-polar solvents. However, calculation of the  $S_1-T_2$  energy gap with the PM3-CAS/CI method seems to be the best way to precisely predict  $\Phi$  values of 4-monosubstituted benzofurazan compounds in non-polar solvents.

#### The effects of the substituent group at the 4-position on the fluorescence quantum yields ( $\Phi$ ) of 4-monosubstituted benzofurazan compounds in polar solvents

As shown in Table 1, the maximum absorption wavelengths of compounds 1–11 were virtually independent of the solvent polarity. In contrast, the maximum emission wavelengths of the six fluorescent compounds were dependent on the solvent polarity. These bathochromic shifts of the maximum fluorescence wavelength were caused by the increase in the dipole moment of the fluorescent 4-monosubstituted benzofurazan compounds in the  $S_1$  state compared to that in the  $S_0$  state

(Table 2). The  $\Phi$  of these compounds were more complicated. The five 4-monosubstituted benzofurazan compounds which were non-fluorescent in non-polar solvents ( $R = H$  (1),  $F$  (8),  $SO_2Me$  (9),  $SO_2Ph$  (10),  $NO_2$  (11)) did not fluoresce even in polar solvents. For the six fluorescent compounds in non-polar solvents, there is a tendency for  $\Phi$  to decrease with an increase in the solvent polarity (Fig. 4). However, the effects of the 4-substituent on  $\Phi$  of the fluorescent compounds are very different. For example,  $\Phi$  of compounds where  $R = NMe_2$  (2) or  $NH_2$  (3) was strongly reduced in highly polar solvents, while that of 6 ( $R = OMe$ ) was not. We tried to elucidate the relationship between  $\Phi$  of compounds 1–11 in polar solvents and the 4-substituent by studying the following points; (i)  $S_1 \rightarrow T_2$  intersystem crossing, (ii) non-radiative relaxation due to formation of hydrogen bonding, (iii) transition to the TICT state, and (iv)  $S_1 \rightarrow T_1$  intersystem crossing.

First, the probability of the  $S_1 \rightarrow T_2$  intersystem crossing was studied. As the  $S_1-T_2$  energy gaps for the optimized  $S_0$  geometry obtained with the PM3-CAS/CI calculation were in good agreement with  $\Phi$  of compounds in non-polar solvents, we considered that a similar relationship might hold in polar solvents. Accordingly, the  $S_1-T_2$  energy gaps at the optimized  $S_0$  geometry in five kinds of solvents were obtained with the PM3-CAS/CI calculation and Onsager's formulations (Fig. 5). Unexpectedly, the  $S_1-T_2$  energy gaps were not changed significantly by the solvent polarity. Based on these results, the probability of the  $S_1 \rightarrow T_2$  intersystem crossing was not changed by the solvent polarity. This explains why these five compounds ( $R = H$  (1),  $F$  (8),  $SO_2Me$  (9),  $SO_2Ph$  (10),  $NO_2$  (11)) did not fluoresce in any solvents. These results also suggest that another non-radiative transition might occur, especially for  $R = NMe_2$  (2) or  $NH_2$  (3), but not for  $R = OMe$  (6), in polar solvents besides the  $S_1 \rightarrow T_2$  intersystem crossing.

Hydrogen bonds can be formed between the benzofurazan compounds and polar solvents, such as alcohol or water. If hydrogen bonding formed between the excited compounds and solvents promotes non-radiative transition,  $\Phi$  dramatically decreases in such protic solvents. Recent papers have

**Table 6** Atomic charges calculated by PM3 calculation

	2	3	4	5	6	7
N at 1-position	-0.159	-0.193	0.083	0.083	-0.250	-0.073
O at 2-position	-0.085	-0.086	-0.063	-0.066	-0.050	-0.075
N at 3-position	0.004	0.072	-0.195	-0.121	0.278	-0.028
Atom connected to the benzofurazan at 4-position	0.337	0.411	0.294	0.435	-0.076	0.227

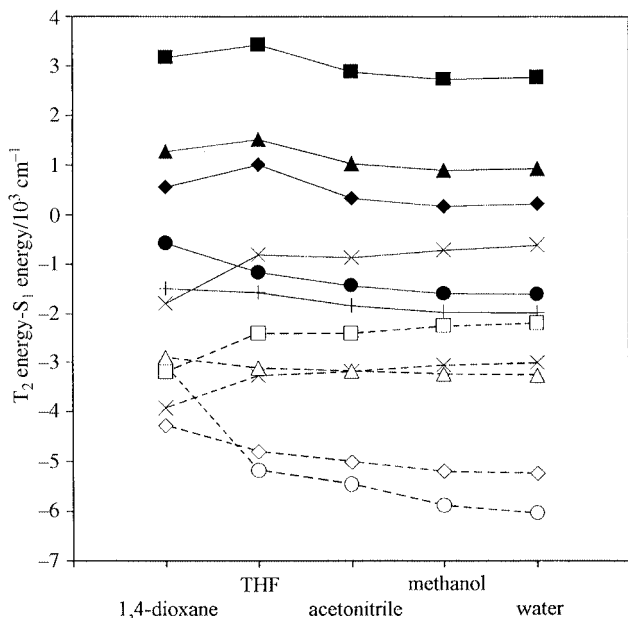


**Fig. 5** Solvent effects on the  $S_1$ - $T_2$  energy gaps, obtained with the PM3-CAS/CI calculation, of 4-monosubstituted benzofurazan compounds; R = H (1,  $\diamond$ , dotted),  $NMe_2$  (2,  $\blacktriangle$ , solid),  $NH_2$  (3,  $\blacklozenge$ , solid),  $SMe$  (4,  $\blacksquare$ , solid),  $SPh$  (5,  $\times$ , solid),  $OMe$  (6,  $+$ , solid),  $NHCOMe$  (7,  $\bullet$ , solid), F (8,  $\circ$ , dashed),  $SO_2Me$  (9,  $\times$ , dashed),  $SO_2Ph$  (10,  $\triangle$ , dashed),  $NO_2$  (11,  $\square$ , dashed). Solvation energies are calculated using eqn. (2).

argued that the formation of hydrogen bonding decreased  $\Phi$  of Coumarin 1<sup>29</sup> or NBD-aminohexanoic acid.<sup>30</sup> To examine whether hydrogen bonding was indeed formed between the 4-substituted benzofurazan compounds and solvents, the atomic charges of nitrogen and oxygen in six fluorescent benzofurazan skeletons were obtained with the PM3 calculation using the optimized  $S_1$  geometry (Table 6). The charge of the atoms binding with the benzofurazan skeleton at the 4-position was also calculated. If the probability of non-radiative relaxation is increased by formation of hydrogen bonding in polar solvents, arrangement of the compounds in order of their ability as hydrogen-bond acceptors should agree with that in descending order of  $\Phi$  caused by the solvent effects, *i.e.*, R =  $NMe_2$  (2) >  $NH_2$  (3) >  $SPh$  (5) >  $SMe$  (4) =  $NHCOMe$  (7) >  $OMe$  (6). Comparing this order with the magnitude of the atomic charges in Table 6, there are no marked relationships. Therefore, we concluded that hydrogen bonding was not the main factor which determined  $\Phi$  of 4-monosubstituted benzofurazan compounds in polar solvents.

The transition from the  $S_1$  state to the TICT state in highly polar solvents is also important for the solvent effects on  $\Phi$ . There are many reports that the transition to the TICT state in highly polar solvents decreased  $\Phi$  of fluorescent molecules.<sup>31-34</sup> Based on previous reports we estimated the probability of the transition to the TICT states using the molecular orbital calculations,<sup>29,33,35</sup> *i.e.*, the  $S_1$  energies for the planar form and the twist form in various solvents of the six fluorescent 4-substituted benzofurazan compounds were obtained with the PM3-CAS/CI calculation (Table 7). As shown in Table 7, the twisting of the substituent group was not favorable, except for R =  $NMe_2$  (2), because the  $S_1$  energy for the twisted form is higher

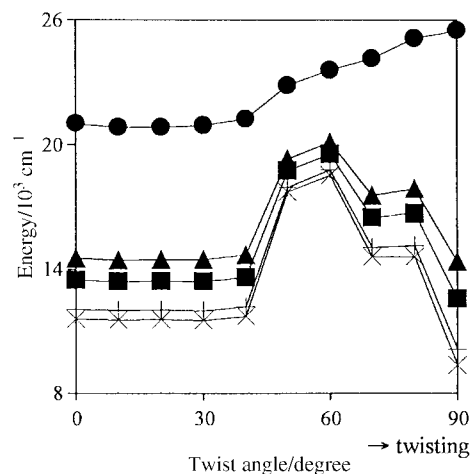


**Fig. 6** Effects of the twisting of the  $NMe_2$  group on the  $S_1$  energy, obtained with the PM3-CAS/CI calculation, of 4-( $N,N$ -dimethylamino)-2,1,3-benzoxadiazole (2) in 1,4-dioxane ( $\bullet$ ), tetrahydrofuran ( $\blacktriangle$ ), acetonitrile ( $\blacksquare$ ), methanol ( $+$ ) or water ( $\times$ ). Solvation energies are calculated using eqn. (1).

than that for the planar form. For R =  $NMe_2$  (2), we obtained the relationship between the  $S_1$  state energy and the twist angle with the detailed PM3-CAS/CI calculations (Fig. 6). Although the perpendicular twisting of the  $NMe_2$  group stabilized the  $S_1$  energy in polar solvents, there were large barriers (about 6000–7000  $cm^{-1}$ ) in the twisting of the  $NMe_2$  group in the  $S_1$  state. The  $\Phi$  of 2 in glycerol was also measured, since this viscous solvent interferes with the transition to the TICT state,<sup>36</sup> and was found to be very low ( $\Phi = 0.00077$ , ab. 430 nm, em. 586 nm). The transition to the TICT state, therefore, does not seem to occur in the  $S_1$  state of 2 in highly polar solvents. In summary, the transition to the TICT state with the twist of the substituent group does not happen in the six fluorescent 4-monosubstituted benzofurazan compounds and is not the factor which determines  $\Phi$  of the 4-monosubstituted benzofurazan compounds in polar solvents.

The probabilities of  $S_1 \rightarrow T_1$  intersystem crossing in polar solvents were finally estimated. Since the dipole moments in the  $S_1$  state are larger than that in the  $T_1$  state of the fluorescent 4-monosubstituted benzofurazan compounds (except for R =  $OMe$  (6) as shown in Table 2, we considered that the  $S_1$  state was close to the  $T_1$  state in these compounds in polar solvents. (The  $S_1$  state was more stabilized than the  $T_1$  state according to eqn. (1) or eqn. (2) of Onsager's formulations.) The  $S_1$ - $T_1$  energy gaps in five solvents at the optimized  $S_1$  geometry were obtained with the PM3-CAS/CI calculations (Fig. 7). Except for R =  $OMe$  (6), the  $S_1$ - $T_1$  energy gaps decreased with solvent polarity. We can relate the change in the  $S_1$ - $T_1$  energy gaps of these compounds with the change in  $\Phi$  value in the polar solvents. The  $S_1 \rightarrow T_1$  intersystem crossing is unfavorable for the fluorescent compounds in non-polar solvents because the  $S_1$ - $T_1$  energy gaps are too large. However, in polar solvents, the  $S_1$ - $T_1$  energy gaps decrease in the compounds which have a large dipole moment in the  $S_1$  state relative to that in the  $T_1$  state. As a result, the probability of the  $S_1 \rightarrow T_1$  intersystem crossing increases and  $\Phi$  of these compounds decreases. As shown in Fig. 7, the  $S_1$ - $T_1$  energy gaps of

**Table 7** Effect of substitutional twisting and solvents on  $S_1$  energy levels

	2	3	4	5	6	7
1,4-Dioxane						
$S_1$ (plane)/ $\text{cm}^{-1}$	21039	20954	24223	26040	25941	23256
$\Delta E S_1$ (to twist)/ $\text{cm}^{-1}$	+4475	+4730	+5022	+4918	+1805	+4897
Tetrahydrofuran						
$S_1$ (plane)/ $\text{cm}^{-1}$	14544	11725	17146	22750	21701	21290
$\Delta E S_1$ (to twist)/ $\text{cm}^{-1}$	-153	+5331	+10537	+7523	+4136	+5686
Acetonitrile						
$S_1$ (plane)/ $\text{cm}^{-1}$	13479	10210	15985	22210	21005	20968
$\Delta E S_1$ (to twist)/ $\text{cm}^{-1}$	-914	+5430	+11442	+7951	+4518	+5815
Methanol						
$S_1$ (plane)/ $\text{cm}^{-1}$	12067	8204	14446	21495	20083	20540
$\Delta E S_1$ (to twist)/ $\text{cm}^{-1}$	-1920	+5560	+12642	+8517	+5025	+5987
Water						
$S_1$ (plane)/ $\text{cm}^{-1}$	11604	7547	13942	21261	19781	20400
$\Delta E S_1$ (to twist)/ $\text{cm}^{-1}$	-2248	+5603	+13034	+8703	+5191	+6043

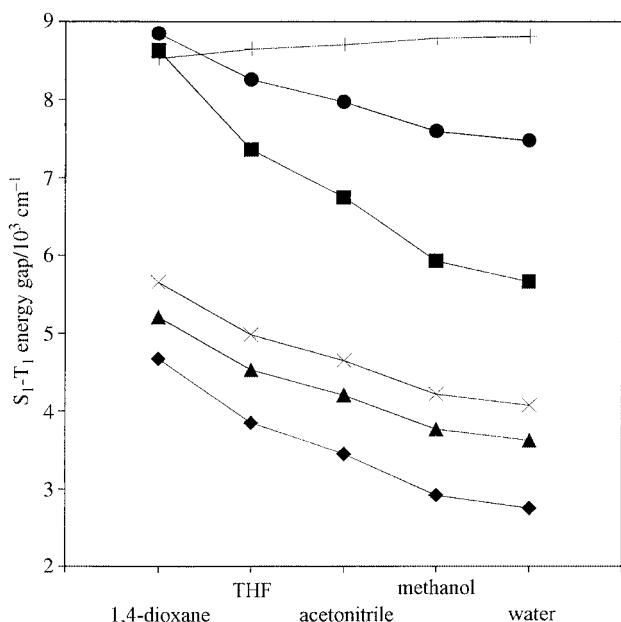


**Fig. 7** Solvent effects on the  $S_1-T_1$  energy gaps, obtained with the PM3-CAS/CI calculation, of fluorescent 4-monosubstituted benzofurazan compounds; R = NMe<sub>2</sub> (2, ▲), NH<sub>2</sub> (3, ◆), SMe (4, ■), SPh (5, ×), OMe (6, +) NHCOMe (7, ●). Solvation energies are calculated using eqn. (1).

compounds with R = NMe<sub>2</sub> (2), NH<sub>2</sub> (3), SMe (4), SPh (5), NHCOMe (7) were smaller in polar solvents than in non-polar solvents. Among these five 4-monosubstituted benzofurazan compounds, the  $S_1-T_1$  energy gaps of compounds with R = NMe<sub>2</sub> (2) and NH<sub>2</sub> (3) in the polar solvents seemed to be small enough for the  $S_1 \rightarrow T_1$  intersystem crossing to occur. Therefore,  $\Phi$  of compounds with R = NMe<sub>2</sub> (2) and NH<sub>2</sub> (3) was dramatically reduced in highly polar solvents compared to non-polar solvents. Although the  $S_1-T_1$  energy gaps of 4, 5 and 7 decreased in polar solvents, the  $S_1-T_1$  energy gaps were larger than those of 2 or 3. Therefore,  $\Phi$  of 4, 5 and 7 was not reduced as much as those of 2 or 3 in the polar solvents. The  $S_1-T_1$  energy gap of 6 was not changed by the solvent polarity. Therefore  $\Phi$  of 6 was not changed even in polar solvents.

We propose a method to predict the fluorescence characteristics of 4-substituted benzofurazan compounds in polar solvents. The effects of the 4-substituent on  $\Phi$  of compounds 1–11

in polar solvents consist of two factors. The first is similar to that in non-polar solvents, the effect on the probability of  $S_1 \rightarrow T_2$  intersystem crossing, which is independent of solvent polarity. The second is the effect on the probability of  $S_1 \rightarrow T_1$  intersystem crossing, which is dependent on solvent polarity. These two factors can be estimated by the PM3-CAS/CI calculations and Onsager's formulations, and therefore, the calculations of the  $S_1-T_2$  and  $S_1-T_1$  energy gaps using the PM3-CAS/CI method and Onsager's formulations must correspond to the effects of the substituent group on  $\Phi$  of 4-monosubstituted benzofurazan compounds in general.

## Conclusion

In this study, the relationships between the fluorescence quantum yields ( $\Phi$ ) of 4-monosubstituted benzofurazan compounds and the substituent groups at the 4-position were obtained. It was indicated that the  $S_1-T_2$  energy gaps obtained with the PM3-CAS/CI calculations related well to  $\Phi$  of the 4-monosubstituted benzofurazan compounds in non-polar solvents. In contrast, in highly polar solvents, the  $S_1-T_2$  and  $S_1-T_1$  energy gaps obtained with the PM3-CAS/CI calculations and Onsager's formulations were in good agreement with  $\Phi$  of the 4-monosubstituted benzofurazan compounds. These results showed that  $\Phi$  of 4-monosubstituted benzofurazan compounds can be predicted by using PM3-CAS/CI calculations and Onsager's formulations. In the future, we will try to prove the obtained relationships by further spectroscopic experiments and elucidate the theoretical relationship between  $\Phi$  of 4,7-disubstituted benzofurazan compounds and the substituent groups at the 4- and 7-positions.

## Experimental

### Materials

Propan-2-ol was obtained from Tokyo Kasei (Tokyo, Japan). Acetone, acetonitrile, benzene, carbon tetrachloride, cyclohexane, dichloromethane, diethyl ether, 1,4-dioxane, ethanol, methanol and tetrahydrofuran were purchased from Kanto Chemicals (Tokyo, Japan). Ethyl acetate and *m*-chloroperbenzoic acid (MCPBA) were obtained from Wako Pure Chemicals (Osaka, Japan). Water was purified using a Milli-Q reagent system (Millipore, Bedford, MA, USA). All chemicals were of HPLC or guaranteed reagent grade and were used without further purification.

## Apparatus

Melting points were measured using a Yanagimoto Micro Melting Point Apparatus (Tokyo, Japan) and are uncorrected. Proton nuclear magnetic resonance ( $^1\text{H-NMR}$ ) spectra were obtained on a JEOL GSX-400 spectrometer (Tokyo, Japan) with tetramethylsilane as the internal standard in  $\text{CDCl}_3$  (abbreviations used: s = singlet, d = doublet and m = multiplet),  $J$  values are given in Hz. Mass spectra were measured using a Hitachi M-1200 H mass spectrometer (atmospheric pressure chemical ionization (APCI) system) (Tokyo, Japan). UV-VIS absorption spectra were measured using a JASCO (Japan Spectroscopic Co., Ltd.) Ubest-50 spectrometer (Tokyo, Japan) in various solvents ( $30 \mu\text{mol l}^{-1}$ ) at room temperature. Fluorescence spectra were measured using a Hitachi F-4010 fluorescence spectrometer (Tokyo, Japan) in fifteen solvents (**4**,  $6 \mu\text{mol l}^{-1}$ ; others,  $30 \mu\text{mol l}^{-1}$ ) at room temperature. Each emission spectrum was obtained by excitation at the maximum absorption wavelength. The fluorescence quantum yields ( $\Phi$ ) were determined using quinine sulfate in  $0.1 \text{ mol l}^{-1}$  sulfuric acid ( $\Phi = 0.55$ , excitation wavelength: 355 nm, room temperature) as the standard.

## Synthesis

2,1,3-Benzoxadiazole (**1**),<sup>37</sup> 4-fluoro-2,1,3-benzoxadiazole (**8**),<sup>38</sup> 4-nitro-2,1,3-benzoxadiazole (**11**)<sup>37</sup> and 4-methoxy-2,1,3-benzoxadiazole (**6**)<sup>39</sup> were synthesized and purified as previously reported.

**4-Amino-2,1,3-benzoxadiazole (3).** 4-Nitro-2,1,3-benzoxadiazole (930 mg, 5.6 mmol) was dissolved in a mixture of dichloromethane (200 ml), conc. hydrochloric acid (12 ml) and methanol (90 ml). After the addition of iron powder (2.13 g), the mixture was vigorously stirred for 25 min at room temperature. The reaction mixture was poured into water (100 ml) and extracted with dichloromethane (150 ml, 3 times). The organic layer was dried over anhydrous sodium sulfate and concentrated *in vacuo*. The residue was chromatographed on silica gel with dichloromethane to afford **3** (618 mg, 81%) as orange needles. Mp: 109–110 °C.  $\delta_{\text{H}}$  ( $\text{CDCl}_3$ ) 7.21 (1H, dd,  $J$  9.0, 7.0), 7.13 (1H, d,  $J$  9.0), 6.35 (1H, d,  $J$  7.0), 4.56 (2H, br). Found: C, 53.49; H, 3.86; N, 31.21. Calc. for  $\text{C}_6\text{H}_5\text{N}_3\text{O}$ : C, 53.33; H, 3.73; N, 31.10%; APCI-MS:  $m/z$  134 ( $(\text{M} - \text{H})^-$ ).

**4-Acetylamino-2,1,3-benzoxadiazole (7).** 4-Amino-2,1,3-benzoxadiazole (41 mg, 0.3 mmol) was dissolved in a mixture of pyridine (2 ml) and acetic anhydride (1.5 ml). The mixture was stirred for 1 h at 80 °C. The reaction mixture was poured into hydrochloric acid ( $1 \text{ mol l}^{-1}$ , 100 ml) and extracted with dichloromethane (100 ml, 3 times). The organic layer was dried over anhydrous sodium sulfate and concentrated *in vacuo*. The residue was chromatographed on silica gel with dichloromethane to afford **7** (44.4 mg, 84%) as a yellow powder. Mp: 162–163 °C.  $\delta_{\text{H}}$  ( $\text{CDCl}_3$ ) 8.26 (1H, d,  $J$  7.0), 8.01 (1H, br), 7.50 (1H, d,  $J$  9.1), 7.41 (1H, dd,  $J$  7.0, 9.1), 2.32 (3H, s). Found: C, 54.25; H, 4.08; N, 23.52. Calc. for  $\text{C}_8\text{H}_7\text{N}_3\text{O}_2$ : C, 54.24; H, 3.98; N, 23.52%; APCI-MS:  $m/z$  176 ( $(\text{M} - \text{H})^-$ ).

**4-(*N,N*-Dimethylamino)-2,1,3-benzoxadiazole (2).** 4-Fluoro-2,1,3-benzoxadiazole (200 mg, 1.4 mmol) was dissolved in 5 ml of acetonitrile. After the addition of dimethylamine solution (40% in water, 1 ml), the mixture was stirred for 2 h at 50 °C. The reaction mixture was evaporated to dryness under reduced pressure and the residue was chromatographed on silica gel with dichloromethane-*n*-hexane (1:1) to afford **2** (230 mg, 98%) as an orange powder. Mp: 33–34 °C.  $\delta_{\text{H}}$  ( $\text{CDCl}_3$ ) 7.24 (1H, dd,  $J$  8.8, 6.8), 7.05 (1H, d,  $J$  8.8), 6.06 (1H, d,  $J$  6.8), 3.32 (6H, s). Found: C, 59.02; H, 5.56; N, 25.90. Calc. for  $\text{C}_8\text{H}_9\text{N}_3\text{O}$ : C, 58.89; H, 5.56; N, 25.75%; APCI-MS:  $m/z$  164 ( $(\text{M} + \text{H})^+$ ).

**4-Phenylthio-2,1,3-benzoxadiazole (5).** 4-Fluoro-2,1,3-benzoxadiazole (118 mg, 0.85 mmol) was dissolved in a mixture of acetonitrile (2 ml), thiophenol (1 ml) and triethylamine (0.4 ml). The mixture was stirred and refluxed for 1 h. The reaction mixture was evaporated to dryness under reduced pressure and the residue was chromatographed on silica gel with *n*-hexane to afford **5** (132 mg, 68%) as a yellow powder. Mp: 82 °C.  $\delta_{\text{H}}$  ( $\text{CDCl}_3$ ) 7.45–7.62 (6H, m), 7.21 (1H, dd,  $J$  8.8, 6.8), 6.80 (1H, d, 6.8). Found: C, 63.24; H, 3.71; N, 12.13. Calc. for  $\text{C}_{12}\text{H}_8\text{N}_2\text{OS}$ : C, 63.14; H, 3.53; N, 12.27%; APCI-MS:  $m/z$  229 ( $(\text{M} + \text{H})^+$ ).

**4-Phenylsulfonyl-2,1,3-benzoxadiazole (10).** 4-Phenylthio-2,1,3-benzoxadiazole (39 mg, 0.17 mmol) was dissolved in 4 ml of dichloromethane. After the addition of MCPBA (141 mg), the mixture was stirred for 1 h at room temperature. The reaction mixture was evaporated to dryness under reduced pressure and the residue was chromatographed on silica gel with ethyl acetate-*n*-hexane (1:3) to afford **10** (34 mg, 76%) as white needles. Mp: 178 °C.  $\delta_{\text{H}}$  ( $\text{CDCl}_3$ ) 8.28 (1H, d,  $J$  5.6), 8.23 (2H, d,  $J$  7.6), 8.10 (1H, d,  $J$  8.8), 7.47–7.65 (4H, m). Found: C, 55.51; H, 3.28; N, 10.71. Calc. for  $\text{C}_{12}\text{H}_8\text{N}_2\text{O}_3\text{S}$ : C, 55.38; H, 3.10; N, 10.76%; APCI-MS:  $m/z$  261 ( $(\text{M} + \text{H})^+$ ).

**4-Methylthio-2,1,3-benzoxadiazole (4).** 4-Fluoro-2,1,3-benzoxadiazole (100 mg, 0.72 mmol) was dissolved in 5 ml of acetonitrile. After the addition of methylsulfanide sodium salt solution (15% in water, 1 ml), the mixture was stirred for 8 h at room temperature. The reaction mixture was evaporated to dryness under reduced pressure and the residue was chromatographed on silica gel with dichloromethane-*n*-hexane (1:1) to afford **4** (85 mg, 71%) as a yellow powder. Mp: 74 °C.  $\delta_{\text{H}}$  ( $\text{CDCl}_3$ ) 7.57 (1H, d,  $J$  9.2), 7.33 (1H, dd,  $J$  9.2, 7.0), 7.03 (1H, d,  $J$  7.0), 2.66 (3H, s). Found: C, 50.51; H, 3.73; N, 16.71. Calc. for  $\text{C}_7\text{H}_6\text{N}_2\text{OS}$ : C, 50.59; H, 3.64; N, 16.86%; APCI-MS:  $m/z$  167 ( $(\text{M} + \text{H})^+$ ).

**4-Methylsulfonyl-2,1,3-benzoxadiazole (9).** 4-Methylthio-2,1,3-benzoxadiazole (52 mg, 0.31 mmol) was dissolved in 5 ml of dichloromethane. After the addition of MCPBA (257 mg), the mixture was stirred for 1 h at room temperature. The reaction mixture was evaporated to dryness under reduced pressure and the residue was chromatographed on silica gel with ethyl acetate-*n*-hexane (2:1) to afford **9** (22 mg, 35%) as yellow needles. Mp: 117 °C.  $\delta_{\text{H}}$  ( $\text{CDCl}_3$ ) 8.20 (2H, m), 7.65 (1H, t), 3.42 (3H, s). Found: C, 42.43; H, 3.13; N, 13.98. Calc. for  $\text{C}_7\text{H}_6\text{N}_2\text{O}_3\text{S}$ : C, 42.42; H, 3.05; N, 14.13%; APCI-MS:  $m/z$  199 ( $(\text{M} + \text{H})^+$ ).

## Computational methods

We employed PM3 (MNDO-Parametric Method 3) for our calculations because this method gave good results for the calculation of the total electron densities on the benzofurazan skeleton and the dipole moment compared with the AM1 (Austin Model 1) method in our previous report.<sup>22</sup> All the PM3 semi-empirical molecular orbital calculations were carried out using the program MOPAC97 in WinMOPAC ver. 2.0 package (Fujitsu, Japan) with a DELL Dimension XPS R450/512K. The geometries of the 4-monosubstituted benzofurazan compounds in the ground state were first completely optimized (keyword PRECISE) by the eigenvector following routine (keyword EF). For several benzofurazan compounds, there was more than one stable conformation. We continued the optimization of these compounds until the lowest energy conformation was found. Similarly, the geometries in the excited state were optimized with the keyword EXCITED in addition to the above keywords. The CAS (Compete Active Space) calculations were then performed on the obtained geometries for calculations of electronic energy, charge distribution and dipole



moment using the configuration interaction with 100 microstates (keywords C.I. = 5 and ISCF). We also calculated the geometry dependence on the ground and excited state energies. The rotation of the substituent groups about its bond in the benzofurazan ring system and the wagging of the benzofurazan skeleton were considered. The electronic energies and dipole moments for these geometries while fixing the angle of the rotation and wagging were likewise obtained with the PM3 and CAS methods fixing the angle. For all calculations of **7**, the keyword MMOK was also used to correct the increase in the barrier to rotation of the amide linkage.

### Solvation energies

The solvent effects on the energy states of the solute were estimated using Onsager's formulations.<sup>35</sup> The solvation energy of the fully relaxed state was calculated using the relation shown in eqn. (1), where  $\mu_i$  represents the dipole moment when

$$\Delta E = -\frac{2\mu_i^2 (\epsilon - 1)}{a^3 (2\epsilon - 1)} \quad (1)$$

the solvent is fully equilibrated,  $a$  is the Onsager cavity radius and  $\epsilon$  is the relative permittivity of the solvent.

When the dipole moment of the solute changes from  $\mu_i$  to  $\mu_f$  very rapidly, the solvent molecules do not have sufficient time to reorient themselves, and one needs to calculate the energy of the partially solvated state. The solvation energy of the partially solvated state was calculated using eqn. (2).

$$\Delta E = -\frac{2}{a^3} \vec{\mu}_f \vec{\mu}_i \left( \frac{\epsilon - 1}{2\epsilon - 1} - \frac{n^2 - 1}{2n^2 - 1} \right) - \frac{2\mu_f^2 (n^2 - 1)}{a^3 (2n^2 - 1)} \quad (2)$$

The energies of the 4-monosubstituted benzofurazan compounds in the ground and excited states in various solvents were calculated using eqn. (3).

$$E(\text{in solvent}) = E(\text{in gas phase}) + (\Delta E(\text{in solvent}) - \Delta E(\text{in cyclohexane})) \quad (3)$$

### Acknowledgements

The authors thank Dr Chang-Kee Lim, MRC toxicology unit, the University of Leicester, for his valuable suggestions and discussion. This work was supported in part by a Grant-in-Aid for Scientific Research from the Ministry of Education, Science and Culture of Japan.

### References

- Y. Ohkura, M. Kai and H. Nohta, *J. Chromatogr., B: Biomed. Appl.*, 1994, **659**, 85.
- A. P. Silva, H. Q. N. Gunaratne, T. Gunnlaugsson, A. J. M. Huxley, C. P. McCoy, J. T. Radmacher and T. E. Rice, *Chem. Rev.*, 1997, **97**, 1515.
- C. E. J. Wheelock, *J. Am. Chem. Soc.*, 1959, **81**, 1348.
- E. M. Kosower, *Acc. Chem. Res.*, 1982, **15**, 259.
- M. G. Neumann, M. H. Gehlen, M. V. Encinas, N. S. Allen, T. Corrales, C. Peinado and F. Catalina, *J. Chem. Soc., Faraday Trans.*, 1997, **93**, 1517.
- R. Saito, T. Hirano, H. Niwa and M. Ohashi, *J. Chem. Soc., Perkin Trans. 2*, 1997, 1711.
- W. M. F. Fabian, K. S. Niederreiter, G. Uray and W. Stadlbauer, *J. Mol. Struct.*, 1999, **477**, 209.
- H. Tomoda, T. Hirano, S. Saito, T. Mutai and K. Araki, *Bull. Chem. Soc. Jpn.*, 1999, **72**, 1327.
- S. Uchiyama, T. Santa, T. Fukushima, H. Homma and K. Imai, *J. Chem. Soc., Perkin Trans. 2*, 1998, 2165.
- K. Imai and Y. Watanabe, *Anal. Chem. Acta*, 1981, **130**, 377.
- T. Toyo'oka, T. Suzuki, Y. Saito, S. Uzu and K. Imai, *Analyst*, 1989, **114**, 413.
- T. Toyo'oka and K. Imai, *Anal. Chem.*, 1984, **56**, 2461.
- K. Imai, T. Toyo'oka and Y. Watanabe, *Anal. Biochem.*, 1983, **128**, 471.
- L. P. Hammett, *J. Am. Chem. Soc.*, 1937, **59**, 96.
- C. Hansch, A. Leo and R. W. Taft, *Chem. Rev.*, 1991, **91**, 165.
- J. J. P. Stewart, *J. Comput. Chem.*, 1989, **10**, 209.
- J. J. P. Stewart, *J. Comput. Chem.*, 1989, **10**, 221.
- S. Uchiyama, T. Santa and K. Imai, *J. Chem. Soc., Perkin Trans. 2*, 1999, 569.
- S. Uchiyama, T. Santa, S. Suzuki, H. Yokosu and K. Imai, *Anal. Chem.*, 1999, **71**, 5367.
- T. Santa, T. Okamoto, S. Uchiyama and K. Imai, *Analyst*, 1999, **124**, 1689.
- A. Toriba, K. Adzuma, T. Santa and K. Imai, *Anal. Chem.*, 2000, **72**, 732.
- S. Uchiyama, T. Santa and K. Imai, *J. Chem. Soc., Perkin Trans. 2*, 1999, 2525.
- V. Bonacic-Koutecky and J. Kohler, *Chem. Phys. Lett.*, 1984, **104**, 440.
- P. Ilich and F. G. Prendergast, *J. Phys. Chem.*, 1989, **93**, 4441.
- W. Rettig, *Angew. Chem., Int. Ed. Engl.*, 1986, **25**, 971.
- W. Rettig and A. Klock, *Can. J. Chem.*, 1985, **63**, 1649.
- R. E. Kellogg, *J. Chem. Phys.*, 1966, **44**, 411.
- R. G. Bennett and P. J. McCartin, *J. Chem. Phys.*, 1966, **44**, 1969.
- G. Saroja, N. B. Sankaran and A. Samanta, *Chem. Phys. Lett.*, 1996, **249**, 392.
- S. Lin and W. S. Struve, *Photochem. Photobiol.*, 1991, **54**, 361.
- J. A. V. Gompel and G. B. Schuster, *J. Phys. Chem.*, 1989, **93**, 1292.
- S. F. Fergues, J. P. Fayet and A. Lopez, *J. Photochem. Photobiol., A*, 1993, **70**, 229.
- T. Soujanya, G. Saroja and A. Samanta, *Chem. Phys. Lett.*, 1995, **236**, 503.
- A. Parusel, *J. Chem. Soc., Faraday Trans.*, 1998, **94**, 2923.
- D. Majumdar, R. Sen, K. Bhattacharyya and S. P. Bhattacharyya, *J. Phys. Chem.*, 1991, **95**, 4324.
- G. Jones II, R. Jackson and A. M. Halpern, *Chem. Phys. Lett.*, 1980, **72**, 391.
- R. J. Gaughran, J. P. Picard and J. V. R. Kaufman, *J. Am. Chem. Soc.*, 1954, **76**, 2233.
- L. D. Nunno, S. Florio and P. E. Todesco, *J. Chem. Soc. C*, 1970, 1433.
- D. D. Monte and E. Sandri, *Ann. Chim., (Rome)* 1964, **54**, 486.